

# Dual-band rectangular microstrip patch antenna at terahertz frequency for surveillance system

Kumud Ranjan Jha · G. Singh

Published online: 3 October 2009  
© Springer Science+Business Media LLC 2009

**Abstract** In this paper, a rectangular microstrip patch antenna on two-layer substrate materials has been analyzed and simulated at the terahertz frequency regime for the surveillance system. The proposed antenna has been simulated at 600 and 800 GHz frequencies by using CST Microwave Studio a commercially available simulator based on finite integral technique. This antenna structure is also simulated by using finite element method based simulator Ansoft HFSS and the results are compared with former.

**Keywords** Rectangular microstrip patch antenna · Microstrip transmission line · Terahertz frequency spectrum · Surveillance systems

## 1 Introduction

TERAHERTZ is the potential frequency regime of the electromagnetic spectrum, which finds its applications in the astronomy, space-science, ultra-fast chemistry and biological imaging [1, 2]. Apart from the space-science, the terahertz spectrum is being explored for the future gigabit indoor wireless communication system [3]. In addition to this,

the terahertz system is also being developed for the surveillance system with the multiple reflectors [4]. It is possible to replace the multiple reflectors surveillance system by the dual-band microstrip antenna based surveillance system in the terahertz frequency spectrum which can be used in scanning an explosive or hazardous materials and provide robust and complete real-time security screening without the need of multiple systems and detection methods. Since the power absorbed by the same material at two frequencies would be different, a comparison of power absorption can be made at these frequencies and the result can be used to compare the available database and predict the nature of material. However, for the successful application of the terahertz spectrum in the wireless or surveillance system, the electrical performances and specially the gain of the microstrip antenna must be enhanced to combat losses due to reflection, refraction and the atmospheric absorption of the terahertz wave.

At the terahertz frequency, the implementation of the antenna is still the matter of research. To enhance the electrical performance of the microstrip antenna at the microwave/millimeter wave frequency regime, photonic crystals as substrate are widely used [5–11]. Brown and Parker [12] have studied the radiation property of microstrip antenna on the photonic crystal substrate. However, these antennas suffer from high radiation losses. Several researchers [13–17] have designed dual-and multi-frequency antennas, which find for suitable applications in wireless communication systems. However, all these designs are restricted to the low frequency regime only. To enhance the performance, multilayer substrate antennas have been studied in detail by [18–21], but they all have again concentrated to the lower frequency (microwave region) only. A simple single frequency THz rectangular patch antenna was reported [22, 23], which suffer from the poor radiation effi-

---

K.R. Jha  
School of Electronics and Communication Engineering, Shri Mata Vaishno Devi University, Katra, Jammu and Kashmir 182301, India  
e-mail: [jhkr@rediffmail.com](mailto:jhkr@rediffmail.com)

G. Singh (✉)  
Department of Electronics and Communication Engineering, Jaypee University of Information Technology, Solan 173215, India  
e-mail: [drghanshyam.singh@yahoo.com](mailto:drghanshyam.singh@yahoo.com)

ciency and the gain. Moreover, the multi-frequency antenna would be more versatile in application on the place of single frequency antenna at terahertz frequency.

To design the antenna at this frequency spectrum, it is necessary to analyze various losses which occur in the terahertz single or multi-frequency antenna. In this paper, a rectangular microstrip patch antenna on two-layer substrate materials for wireless/surveillance systems has been analyzed and simulated. Several types of losses such as dielectric and conduction at the terahertz frequency regime for a two-layer substrate material are also investigated and then used to design a single and dual-band microstrip patch antenna for aforementioned applications. The organization of this paper is as follows. Section 2 concerns with the analysis of various types of losses and design optimization of the proposed two-layer substrate rectangular microstrip patch antenna at terahertz frequency. Section 3 discusses about the simulated results of the proposed antenna. Finally, Sect. 4 concludes the work.

## 2 Analysis

The geometrical configuration of the proposed two-layer substrate material based rectangular microstrip patch antenna is shown in Fig. 1. The electrical performance of any single port microwave component such as microstrip antenna is greatly influenced by the conductor loss, dielectric loss and return loss. Among these losses, return loss is associated with the matching condition of device with the port. However, other two losses are dependent on the selection of substrates and conductors of the antennas. These losses are proportional to the frequency of the operation. At the terahertz electromagnetic spectrum, where frequency is quite high in comparison to microwave frequencies, it is required

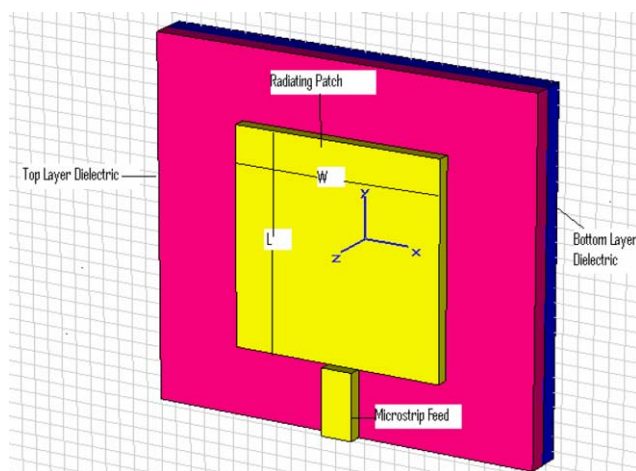


**Fig. 1** Geometrical configuration of the rectangular microstrip patch antenna on two-layer substrate materials

to consider these losses for the selection of materials and the design of antennas. As we know, at the terahertz frequency the skin-depth of the conductors (ground and radiator) is very small hence the conductor loss is very high. In order to make proper selection of the material, we have analyzed conductor and dielectric losses of the proposed antenna in detail before proceeding to the actual design of it.

### 2.1 Loss estimation of proposed antenna

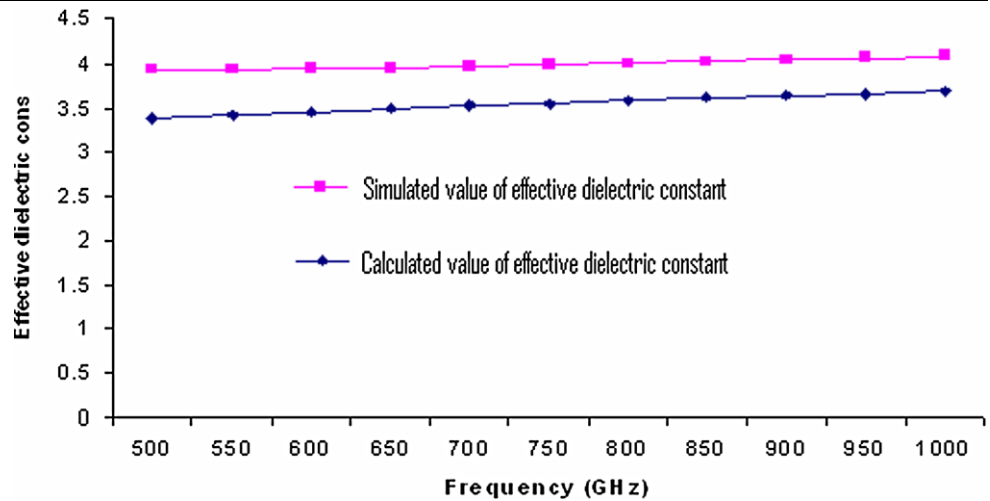
The proposed antenna is designed on the two-layer dielectric substrate materials in which the thickness of each layer is 25  $\mu\text{m}$ . The dielectric permittivity of the layer of the substrate materials on the ground plane is  $\epsilon_2 = 3.2$  with loss tangent 0.003. This layer is followed by layer of dielectric permittivity  $\epsilon_1 = 6.0$  of loss tangent 0.0035. The radiating patch and the microstrip feed lines are made of copper ( $\sigma = 5.8 \times 10^7 \text{ S/m}$ ). The width of feed line is 40  $\mu\text{m}$ . Microstrip line feed has been used in the proposed antenna which is one of the most commonly used feeding techniques. In this feeding technique, a conducting strip is connected directly to the edge of the rectangular patch microstrip antenna. The advantage of this technique is that both the feed and patch lie on the surface of the substrate and therefore is plane in construction and provide the right impedance match between the patch and feed line. Based on these parameters dielectric and conductor losses have been analytically calculated and compared with the simulation results and discussed in subsequent paragraphs.

#### 2.1.1 Dielectric loss

Dielectric loss is the frequency dependent quantity at the high frequency. Due to the dependence on the frequency, dielectric permittivity of the material also changes. Therefore, before designing any microstrip device in the terahertz frequency range, the first task is to estimate effective dielectric permittivity of the material. However, there is no such direct formula to calculate this frequency dependent dielectric permittivity of the material at terahertz frequency. A formula was suggested in [24] but application of this formula is a tedious task. Moreover, the accuracy of this formula at THz frequency is not verified. The problem of calculation aggravates when multiple dielectric layers are used in the microstrip antenna design. To calculate the effective dielectric permittivity, it is required to calculate the relative dielectric permittivity of the composite ( $\epsilon_{rc}$ ). This value has been calculated using two-capacitance model, which indicates that two stacked dielectric layers can be modeled as two capacitances in series and net capacitance is equal to:

$$C = \frac{C_1 C_2}{C_1 + C_2} \quad (1)$$

**Fig. 2** The comparison of an effective dielectric constant of the two-layer substrate materials



where  $C, C_1, C_2$  are total capacitance, capacitance of the dielectric layer below the radiating patch and above the ground plane dielectric materials, respectively. Since the capacitance is directly proportional to the dielectric permittivity and inversely proportional to distance between two plates, the relative dielectric permittivity of the composite material is calculated as:

$$\epsilon_{rc} = \frac{d\epsilon_1\epsilon_2}{d_2\epsilon_1 + d_1\epsilon_2} \tag{2}$$

where  $d, d_1, d_2$  are total, substrate layer below the radiating patch and substrate layer above the ground plane thickness, respectively. The calculated value of  $\epsilon_{rc}$  in the present case is equal to 4.173. The frequency dependent effective dielectric permittivity  $\epsilon_{re}$  of the material is calculated using PCAAD21 calculator (Sintel Legacy Co.), which is based on the full-wave analysis. The result is compared by simulating the structure with the CST Microwave Studio a commercially available simulator. The comparisons of the two results are shown in Fig. 2.

Figure 2 shows a close agreement between two results. The nature of the graph in both cases is same. Only a deviation of about 0.6 is seen in two cases as shown in Fig. 2. This deviation is attributed by two reasons. Firstly, in the calculation a truncation error after three decimal points has occurred and secondly, the CST Microwave Studio simulator works on finite integral technique where as calculation has been based on the full-wave analysis. After calculating the effective dielectric permittivity at different frequencies, dielectric attenuation constant, index of attenuation loss is calculated using the formula mentioned below [25]:

$$\alpha_d = 27.3 \left( \frac{\epsilon_{rc}}{\epsilon_{re}} q \right) \frac{\tan \theta}{\lambda_g} \frac{dB}{\lambda_g}, \tag{3}$$

where  $q = \left( \frac{\epsilon_{re}-1}{\epsilon_{rc}-1} \right)$  is the filling factor. In (3)  $\tan \theta$  and  $\lambda_g$  are loss tangent and guided wavelength, respectively. It is clear

from the ongoing discussion that loss tangent also varies due to change in the effective dielectric permittivity. Since the  $\tan \theta = (\epsilon''/\epsilon') \cong \delta_l$  and  $\epsilon = \epsilon' - j\epsilon''$ . The composite dielectric  $\epsilon_{rc}$  in the present case can be equated to:

$$\epsilon_{rc} = \frac{d(\epsilon'_1 - j\epsilon''_1)(\epsilon'_2 - j\epsilon''_2)}{d_1(\epsilon'_2 - j\epsilon''_2) + d_2(\epsilon'_1 - j\epsilon''_1)}. \tag{4}$$

From (4) it is seen that the loss tangent is also a frequency dependent quantity. In order to simplify the design, loss tangent of both materials are approximated to the same value (0.003). Based on the above assumptions, dielectric attenuation constant ( $\alpha_d$ ) has been calculated. To validate the result, dielectric quality factor  $Q_d$  is extracted from the simulated result and  $\alpha_d$  is calculated using formula mentioned below:

$$\alpha_d = \frac{27.3}{Q_d} \frac{dB}{\lambda_g}. \tag{5}$$

Analytical and simulated results are shown in Fig. 3. The result shows a close agreement between simulated and calculated values. It implies that this technique can be extended to other terahertz frequency to calculate the dielectric loss.

### 2.1.2 Conductor loss

Normally, conductor’s surface skin resistance increases with increase in frequency. Increased surface resistance leads to increased loss of power due to skin effect. To overcome this problem, thickness of conducting material should be at least three times higher than skin depth. In the present case, the calculated skin depth is equal to 0.09  $\mu\text{m}$  at 500 GHz. In order to make the circuit practically realizable the conductor (Copper) of thickness 17  $\mu\text{m}$  is taken in to the account. The conductor attenuation constant ( $\alpha_c$ ) is calculated using the

**Fig. 3** The comparison of dielectric attenuation constant

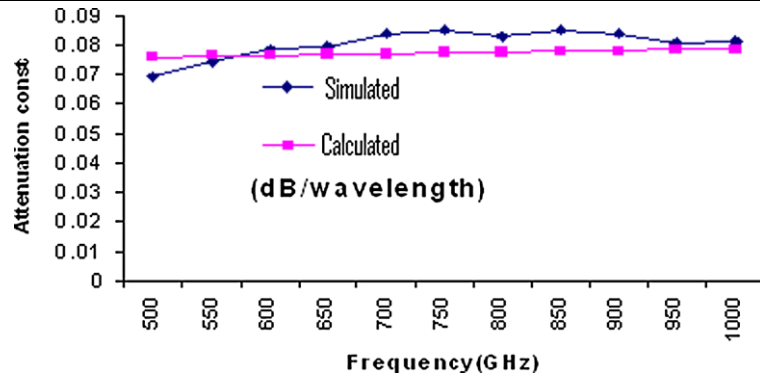
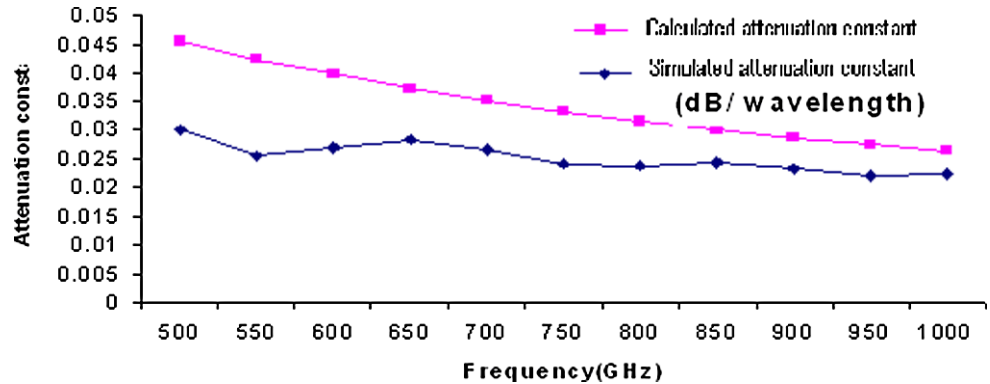


**Fig. 4** The comparison of conductor attenuation constant



formula [26]:

$$\frac{\alpha_c Z_0 h}{R_s} = \frac{8.68}{2\pi} \left[ 1 - \left( \frac{w'}{4h} \right)^2 \right] \left[ 1 + \frac{h}{w'} + \frac{h}{w'} \left( \ln \frac{2h}{t} - \frac{t}{h} \right) \right]$$

for  $\frac{1}{2\pi} < \frac{w}{h} \leq 2$

where  $w' = w + \Delta w$ , and

$$\Delta w = \frac{t}{\pi} \left( \ln \frac{4\pi w}{t} + 1 \right) \quad \text{for } \frac{2t}{h} \leq \frac{w}{h} \leq \frac{\pi}{2} \quad (6)$$

where  $w$  is the width of microstrip line,  $t$  is the total conductor thickness, and  $Z_0$  is characteristic impedance of microstrip transmission line.  $\alpha_c$  is expressed in dB/cm. Again, to validate the result obtained analytically, the simulated conductor quality factor ( $Q_c$ ) is extracted. Two results are rationalized in same unit (dB/guided wavelength). The comparison of result is shown in Fig. 4. Both results are in close agreement and attenuation constant due to conductor can be calculated in this manner.

### 2.2 Physical dimensions of proposed antenna

In the previous section various losses of the substrate and patch materials have been estimated which reveals that these losses and critical parameters are minimum in the terahertz frequency band from 500–1000 GHz. Due to the low loss of the energy within the substrate and metallization, it is

expected that the antenna designed on this substrate combination would yield high electrical performance. The physical dimensions of resonator and feed line can be calculated analytically on any substrate and antenna can be designed. However, the practical antenna should be an efficient radiator. Moreover, the dimension and loss depend on thickness and relative permittivity of material. In the present investigation, as losses are negligible, the enhanced electrical performance antenna design is possible with the help of this material. Due to reduced permittivity, the size of the patch is increased reasonably to reduce the fabrication error.

#### 2.2.1 Calculation of physical dimensions

At the first hand, approximate physical dimensions of radiating microstrip patch have been calculated using following formulas:

$$W = \frac{1}{2f_r \sqrt{\epsilon_{re} \mu_0 \epsilon_0}} - 2\Delta W, \quad (7)$$

$$L = \frac{1}{2f_r \sqrt{\mu_0 \epsilon_0}} \sqrt{\frac{2}{\epsilon_{rc} + 1}} \quad (8)$$

where

$$\frac{\Delta W}{h} = 0.42 \frac{(\epsilon_{re} + 0.3) \left( \frac{L}{h} + 0.264 \right)}{(\epsilon_{re} - 0.258) \left( \frac{L}{h} + 0.8 \right)}. \quad (9)$$

**Fig. 5** An equivalent circuit model of the radiating patch

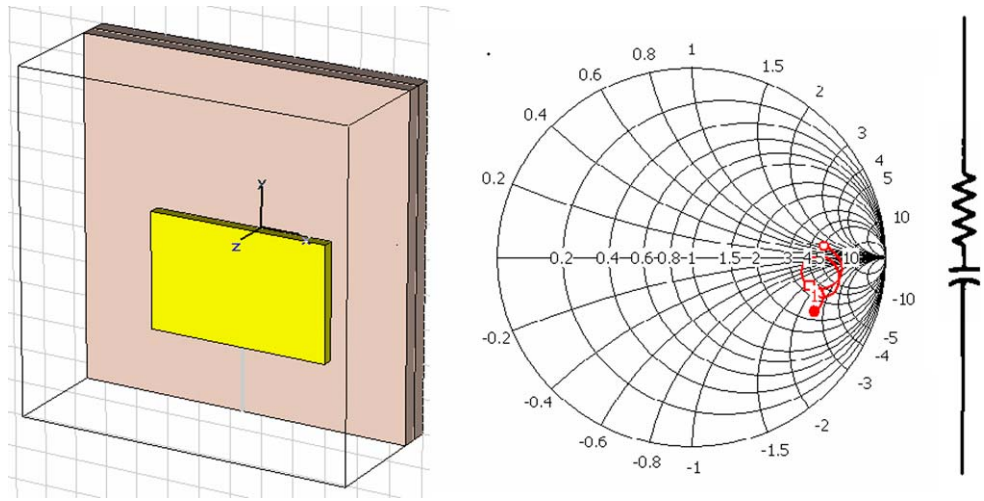
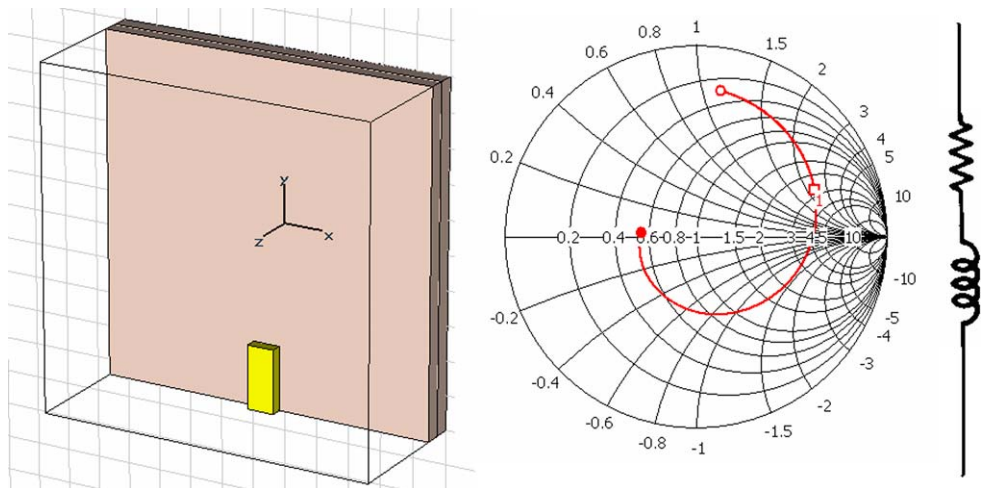


**Fig. 6** An equivalent circuit model of the microstrip feed-line



Based on the above design formulas, the values of length and width ( $L$  and  $W$ ) of the radiating patch have been calculated at resonance frequency 600 GHz and they are 155  $\mu\text{m}$  and 82  $\mu\text{m}$ , respectively. However, the result is not optimum. The return loss is below  $-10$  dB for wide band of signal and resonance condition is not achieved. It is due to parasitic value of capacitance and inductance at the frequency of interest. To optimize the result, it is required to optimize  $L$ ,  $W$ , and feed position.

### 2.2.2 Optimization of structure

From the structure, it is seen that behavior of rectangular patch is capacitive in nature since the width of this is greater than the width at characteristic impedance of port ( $50 \Omega$ ), which is further verified by simulating the structure alone. For the simulated structure, its input impedance when excited by  $50 \Omega$  port and equivalent circuit model is shown in Fig. 5.

On the same way, the microstrip feed line is modeled as inductive circuit since the width of the feed line is lesser than

characteristic impedance width of the port ( $50 \Omega$ ) at same substrate. The Smith-chart of this structure along with its equivalent circuit model is shown in Fig. 6.

Extracted values of the input impedances seen by port of two circuits are equal to  $173 - j87.47 \Omega$  and  $189.5 + j168.2 \Omega$ , respectively. When these impedances are connected directly, the resultant impedance is equal to  $362.5 + j80.73 \Omega$ . This result indicates that to achieve the resonance condition a series capacitance must be added so that imaginary part of the impedance would become zero at the resonance frequency. The resistive part of the circuit would only account for loss and it would affect the return loss. In order to achieve the resonance condition at 600 GHz, a series capacitance between feed line and rectangular patch is added. The whole structure is modeled as the circuit shown in Fig. 7.

Finally, the structure has been optimized by varying  $L$ ,  $W$  and feed position. The final dimension of the structure is shown in Table 1.

It is interesting to note that the width of the radiating patch is approximately equal to  $\lambda_0/2$  which behaves as the perfect resonator.

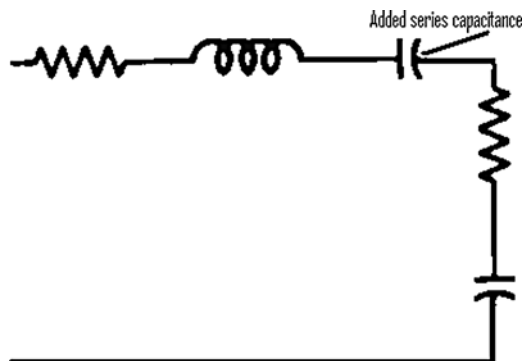


**Fig. 7** Equivalent circuit model of structure

**Table 1** Dimensions of the structure

Parameter	Value
Ground	Perfect conductor
Upper/Lower layer substrate length	500 $\mu\text{m}$
Upper/Lower layer substrate width	500 $\mu\text{m}$
Length of radiating patch ( $L$ )	170 $\mu\text{m}$
Width of radiating patch ( $W$ )	270 $\mu\text{m}$
Length of microstrip feed line	93.337 $\mu\text{m}$
Width of microstrip feed line	40 $\mu\text{m}$
Series gap between feed and patch	6.667 $\mu\text{m}$
Thickness of each substrate	25 $\mu\text{m}$

### 3 Results and discussion

The simulated value of scattering parameter by using CST Microwave Studio and Ansoft HFSS simulator is shown in Fig. 8.

It is clear from Fig. 8 that the return loss of the structure is better than  $-30$  dB and  $-10$  dB impedance bandwidth of the proposed antenna is 12.85% at 600 GHz when simulated using CST Microwave Studio. The  $-10$  dB impedance bandwidth of the same structure is equal to 10.9% when simulated by using Ansoft HFSS. A discrepancy in the result is due to the simulation technique, application of perfect electric conductor in place of copper and the application of the lumped port of  $50 \Omega$  characteristics impedance in the second simulator (HFSS). However, the discrepancy in desired band of the operation is less and it validates the proposed structure to work as an efficient antenna. Since the dimension of the structure is comparable to the wavelength, far-field radiation pattern is achievable. The far-field radiation pattern of the structure is shown in Fig. 9. The radiation efficiency of this structure is 79.7%. The gain and directivity of this antenna are equal to 9.8 dB and 10.7 dBi, respectively.  $-3.0$  dB beam widths in E and H plane are  $38.4^\circ$  and  $47.8^\circ$ , respectively.

In the previous analysis, microstrip feed line was aligned to the centre of width of the radiating patch as shown in Fig. 1. It is seen from Fig. 8 that in addition to resonance at 600 GHz, there is dip in return loss below  $-10$  dB near 800 GHz. The real part of the input impedance of structure seen by port is near  $50 \Omega$  around 600 and 800 GHz. Due to which the return loss is reduced below  $-10$  dB near 800 GHz, which can be utilized in designing two-frequency antenna. The cavity model of this structure is shown in

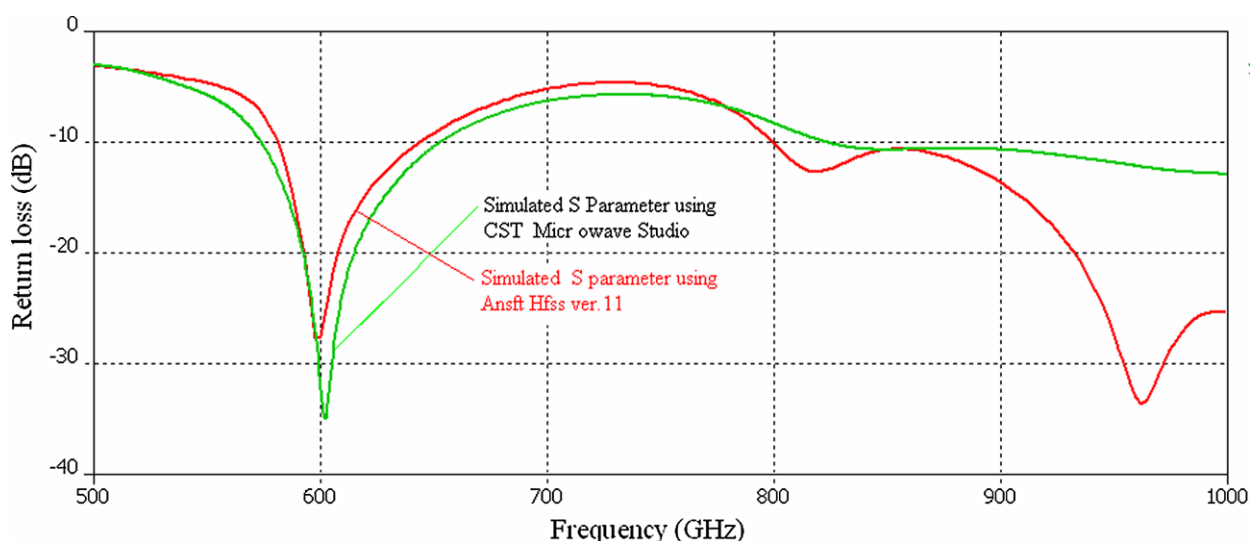


**Fig. 8** The frequency characteristics of the return loss (in dB) of the proposed microstrip antenna on two-layer substrate materials

Fig. 10. It is seen from Fig. 1 that the feed line is not directly loading to the radiating patch, so the transformation of this structure in to equivalent circuit as shown in Fig. 10

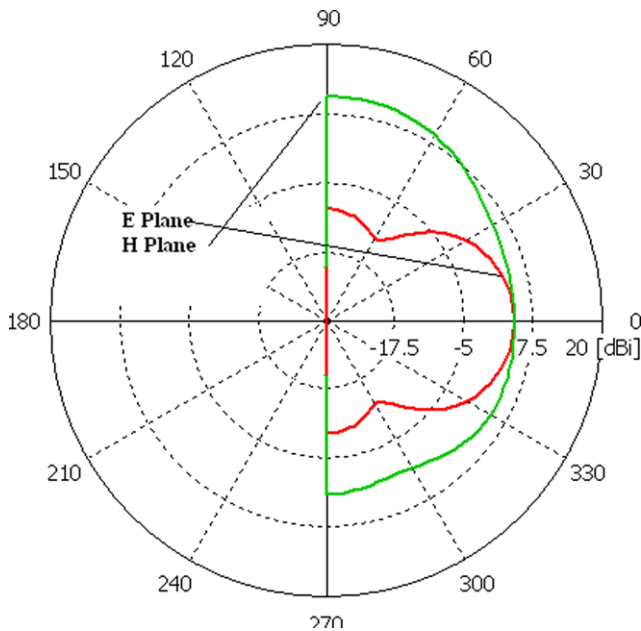


Fig. 9 The radiation characteristics in principle planes of the proposed antenna at 600 GHz

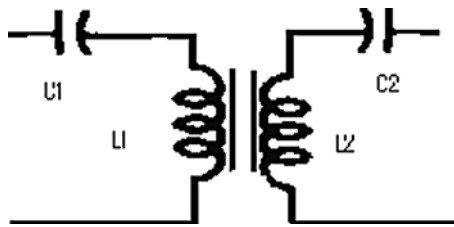


Fig. 10 An equivalent cavity model of the proposed antenna

is a reasonable choice under symmetric/asymmetric loading of the structure.

From Fig. 10, it is seen that two self-resonance frequencies of the structure is possible due to the unequal current and voltage distribution in the left and right of the  $y$  axis of feed-line (neglecting the coupling coefficient). In order to achieve two resonance conditions, the length ( $L$ ) and feed position have been varied while fixing the width ( $W$ ) equal to  $270 \mu\text{m}$ . The effect of variation in patch length is shown in Fig. 11.

To optimize the result at two frequencies, the lower boundary of length ( $L$ ) is fixed at  $y_{\text{min}} = -150 \mu\text{m}$  in the rectangular coordinate system while keeping the width ( $W$ ) fixed with upper and lower end points at  $x_{\text{min}} = -135$  and  $x_{\text{max}} = 135 \mu\text{m}$ . On this way the width of the structure is same as shown in Table 1 and it is equal to  $270 \mu\text{m}$ . To see the effect of variation in the length of the proposed structure, a parameter ‘ $a$ ’ is selected on the  $y$  axis and the effect of the variation in the parameter ‘ $a$ ’ is observed in Fig. 11. The structure exhibits dual resonance condition for the value of ‘ $a$ ’  $\geq 111.429 \mu\text{m}$ . In other words, the structure resonates at two different frequencies for the value of  $L \geq 261 \mu\text{m}$ . For the value of  $a = 157.143 \mu\text{m}$ , two sharp resonances at 600 and 800 GHz are clearly visible in Fig. 11. For this value of ‘ $a$ ’, the length of the structure is equal to  $307.143 \mu\text{m}$ . At this value of ‘ $a$ ’ the resonance shifts slightly below 800 GHz. To tune the structure to resonate at 800 GHz, the optimum value of ‘ $a$ ’  $= 150 \mu\text{m}$  is considered in the present design. With this value of optimization parameter, the length of the structure is fixed to  $300 \mu\text{m}$ . After fixing this value, to enhance the performance of the antenna, the feed position from the initial value of  $x_{\text{min}} = -20 \mu\text{m}$  is shifted in the positive direction. This shift in the feed position on the  $x$ -axis causes the return loss pattern to change

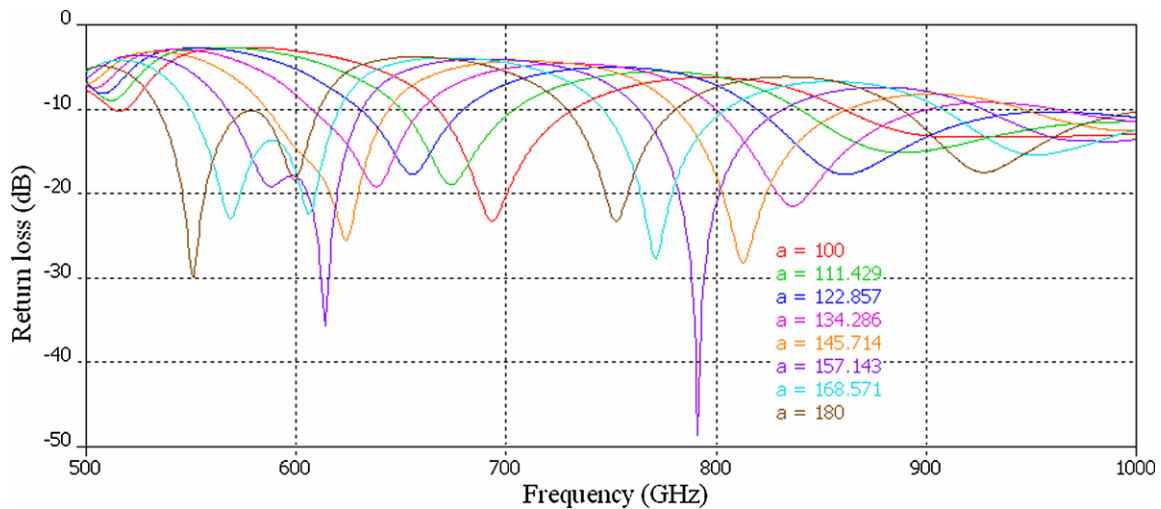
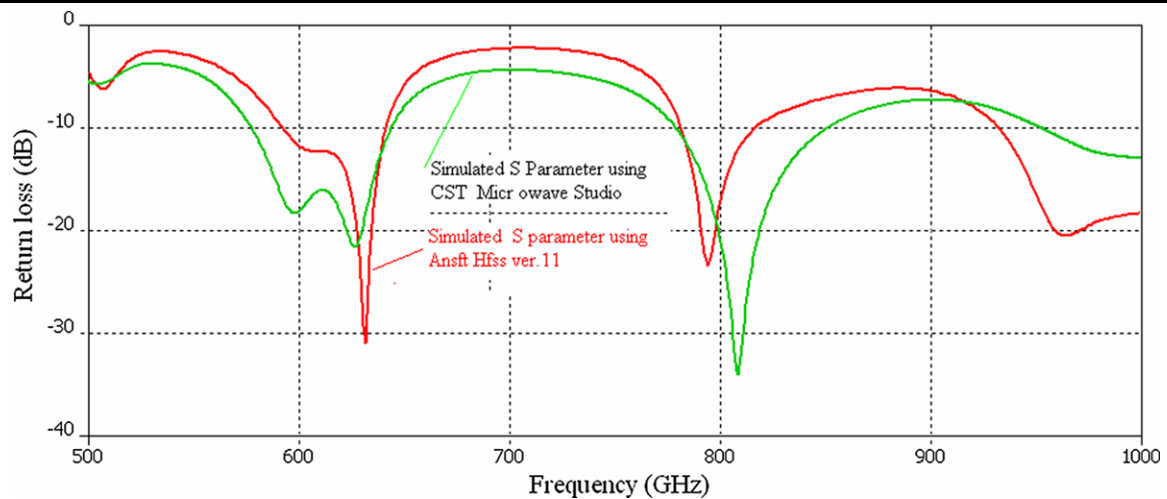


Fig. 11 An optimization of the length of the radiating patch



**Fig. 12** Frequency characteristics of the return loss (in dB) from two different simulation packages

**Table 2** Dimensions of structure

Parameter	Value
Ground	Perfect conductor
Upper layer substrate size	$500 \times 500 \mu\text{m}^2$
Lower layer substrate size	$500 \times 500 \mu\text{m}^2$
Length of radiating patch ( $L$ )	$300 \mu\text{m}$
Width of radiating patch ( $W$ )	$270 \mu\text{m}$
Length of microstrip feed line	$93.337 \mu\text{m}$
Width of microstrip feed line	$40 \mu\text{m}$
Series gap between feed and patch	$6.667 \mu\text{m}$
Thickness of each substrate	$25 \mu\text{m}$
Feed position	$-18$ to $22 \mu\text{m}$ on $x$ axis

due to the asymmetric loading of the feed-line on the resonator. When the feed position is varied with distance, the resonance position on the frequency axis shifts to the extreme position on the frequency axis. To centre around the intended frequencies of 600 and 800 GHz, the feed position is shifted by  $2 \mu\text{m}$ . Since this shift is insignificant, the variation against the feed position is not presented in this work. The change in the resonance condition is attributed to the change in the inductive and capacitive parameters of the circuit model as shown in Fig. 10. Finally, the optimized parameter values are shown in Table 2.

The return loss response of the proposed antenna for the optimized physical parameters is shown in Fig. 12. It is seen from the response that  $-10$  dB fractional bandwidth (FBW) of the structure at two resonant frequencies (600 and 800 GHz) are 10.49 and 8.90%, respectively when simulated by using CST Microwave Studio. In the second case of simulation by using Ansoft HFSS, FBW is 8.33 and 3.33%, respectively. The variation in result is expected due to simulation technique involved. However, it is seen from Fig. 12

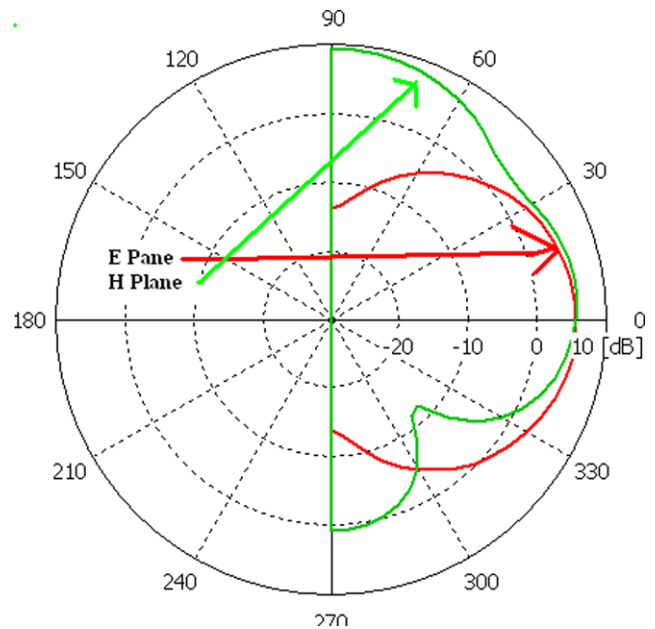


**Fig. 13** The gain characteristics of proposed antenna in E and H plane at 600 GHz

that the return loss is in the close agreement in both cases of simulation at 600 GHz 800 GHz. It indicates that the proposed structure will radiate the energy at these two frequencies. Radiation pattern of the proposed antenna at 600 and 800 GHz is shown in Fig. 13 and Fig. 14, respectively.

In Figs. 13 and 14, the red and blue lines indicate E and H plane, respectively. The electric performance of the proposed dual-frequency microstrip patch antenna obtained by simulating the structure in different software at 600 and 800 GHz are presented in Table 3. The gain of the dual-frequency antenna at 600 GHz is identical to the single frequency antenna. Only a small drop in the gain equal to 0.23 dB is noticed from Fig. 9 and Fig. 13. This variation is

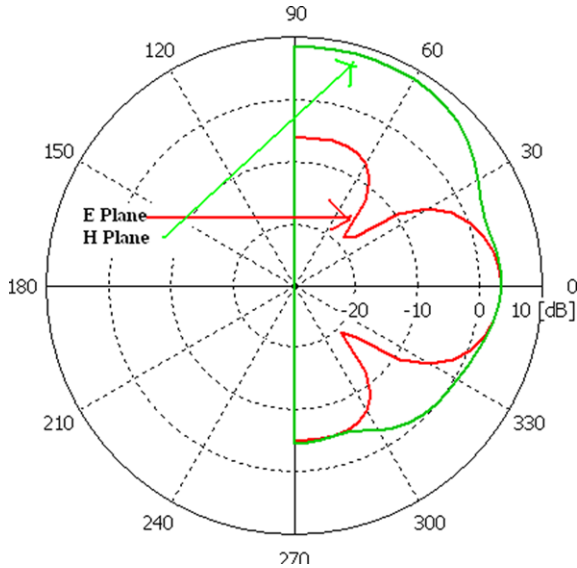


**Fig. 14** The gain characteristics of the proposed microstrip patch antenna in E and H plane at 800 GHz

due to the shift in the return loss pattern at this frequency as shown in Fig. 8 and Fig. 12.

For the potential application of such a dual-band microstrip antenna at the terahertz frequency, the orientation of co-polarized and cross-polarized field at these frequencies (600 and 800 GHz) are investigated. To observe the pattern, the proposed antenna is simulated by using two different simulators at two azimuth angles ( $\phi = 0^\circ$  and  $\phi = 90^\circ$ ) and the elevation angle is varied in  $1^\circ$  step in the range of  $-90^\circ \leq \theta \leq 90^\circ$ .

From Fig. 15(a) it is seen that the gain of co-polar field component is maximum in  $xz$  plane ( $\phi = 0^\circ$ ) at  $\theta = 0^\circ$

**Table 3** Radiation parameters at dual frequency

Parameter	At 600 GHz		At 800 GHz	
	CST	HFSS	CST	HFSS
Radiation efficiency	83.86%	96.10%	84.50%	95.70%
Gain	9.57 dB	10.90 dB	8.58 dB	9.13 dBi
Directivity	10.34 dBi	11.40 dBi	9.31 dBi	9.44 dBi

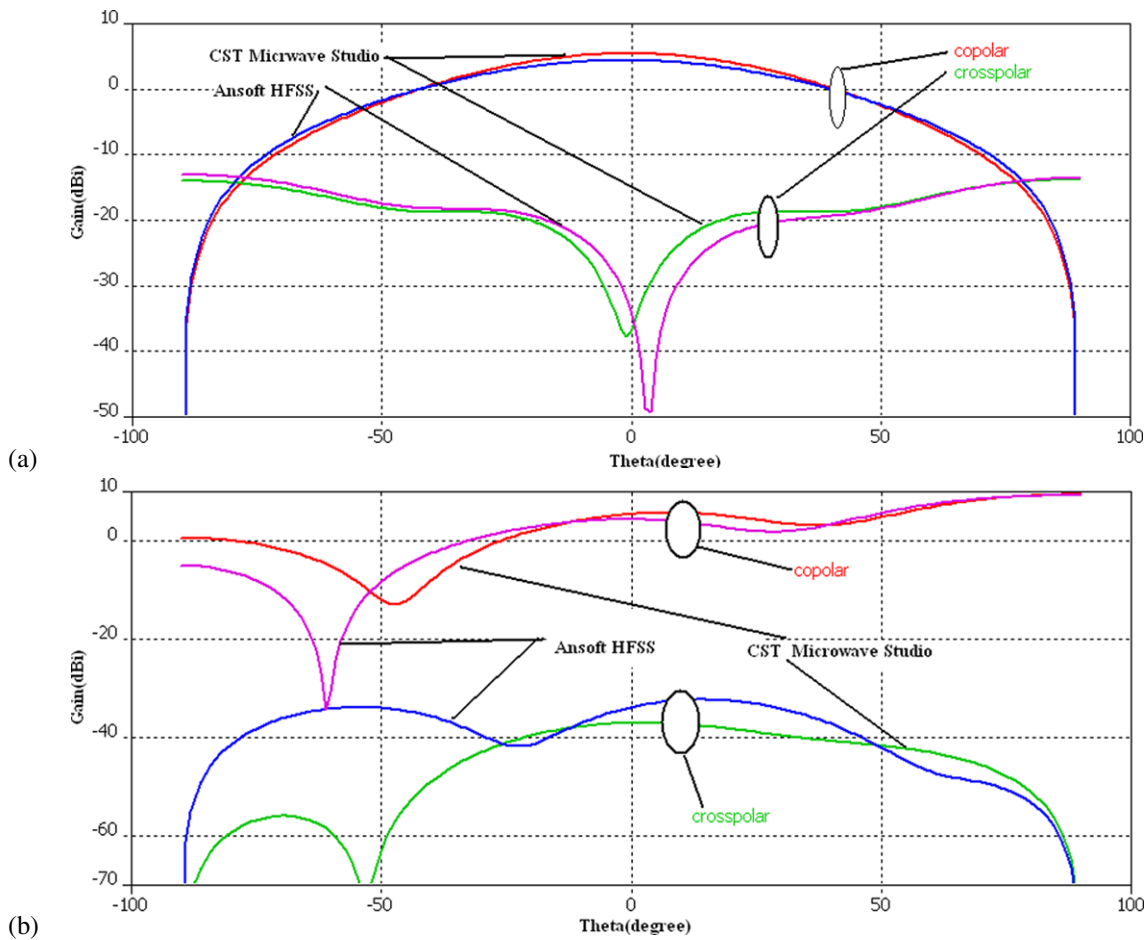


**Fig. 15** Polarization of the antenna at 600 GHz (a) at  $\phi = 0^\circ$ , and (b) at  $\phi = 90^\circ$

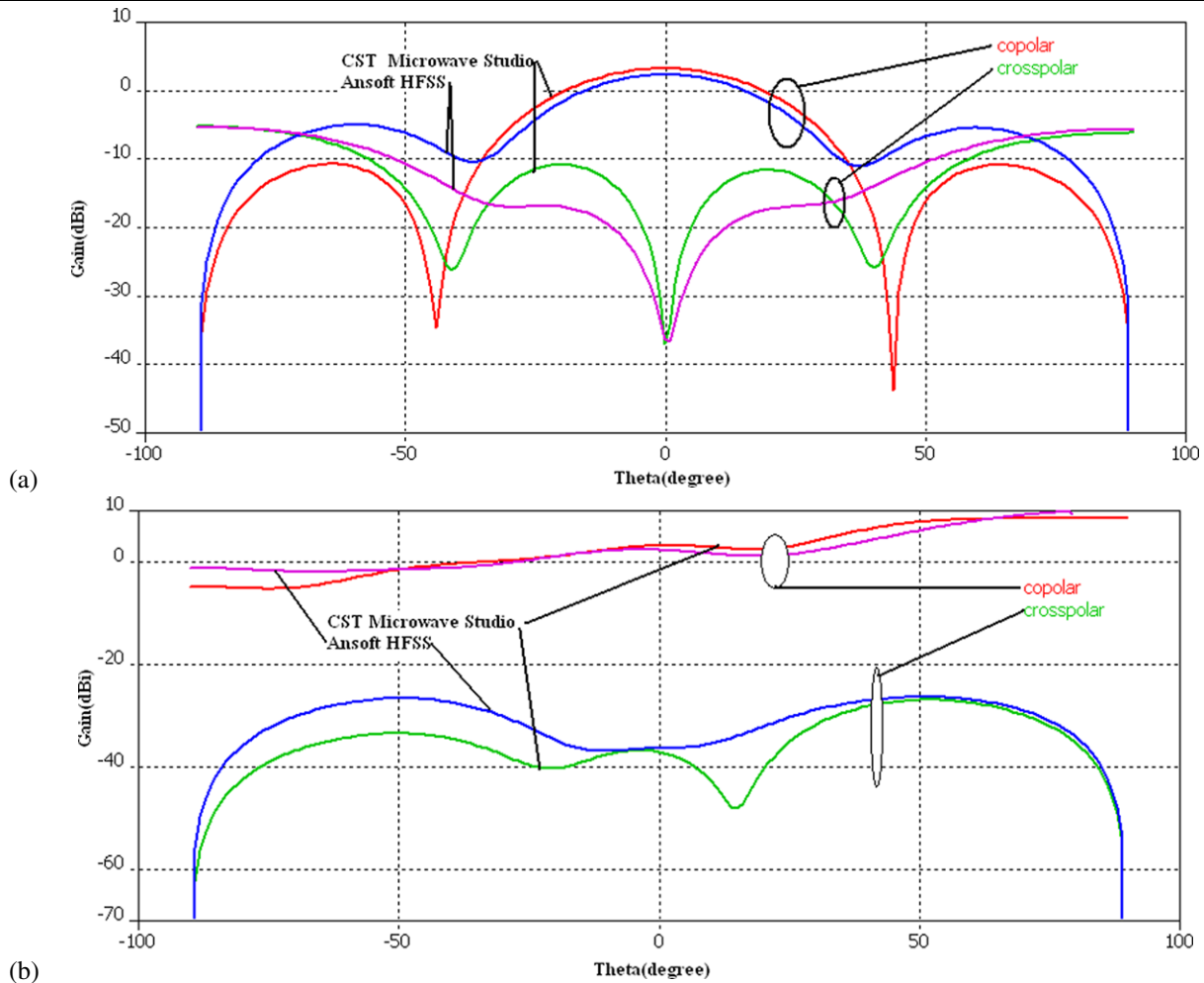


**Fig. 16** Polarization of the antenna at 800 GHz (a) at  $\phi = 0^\circ$ , and (b) at  $\phi = 90^\circ$

(5.5 dBi) and the cross-polarization is about  $-35$  dB at this point. The cross-polarized field is below  $-15$  dBi in the range of  $-90^\circ \leq \theta \leq 90^\circ$ . In the  $yz$  plane ( $\phi = 90^\circ$ ), the co-polarization maximum gain is about 9.5 dBi at  $\theta = 90^\circ$  and approaches to the absolute gain of the antenna. The cross-polarization level is below  $-35$  dBi in the range of  $-90^\circ \leq \theta \leq 90^\circ$ . The simulated results obtained by using both simulators are in the close agreement.

The effect of polarization of the same antenna at 800 GHz is shown in Fig. 16(a) and (b). Results at this frequency is identical to results obtained in Fig. 15, except a variation in the co-polarization of the field in the  $xz$  plane in which co-polarized field decreases around  $\theta = \pm 44^\circ$ . However, the cross polarization of the field is below  $-6.0$  dBi even in the worst case. In the  $yz$  plane ( $\phi = 90^\circ$ ), the co-polarization is maximum and approaches to the absolute of the antenna at  $\phi = 90^\circ$  which is about 10.0 dBi. This investigation indicates the applicability of the antenna at two different frequencies in which field orientation is similar at  $\phi = \theta = 90^\circ$ .

#### 4 Conclusion

In this paper, a rectangular microstrip antenna on two-layer substrate materials has been analyzed and simulated. Various losses at terahertz frequency range have been analytically calculated and compared with the simulation. The antenna feeding technique has been dealt in detail and with the help of series-loaded capacitance the response at 600 and 800 GHz has been optimized. In the case of single resonance condition, radiation efficiency upto 79.7% has been achieved. The gain and directivity of this antenna is equal to 9.8 dB and 10.7 dBi, respectively. Further, the same patch has been tuned in dimension to behave as the dual-band antenna. The antenna in both cases exhibits excellent radiation efficiency, gain and directivity. Apart from the possible future application in the wireless communication/surveillance system already discussed above, the comparison of electrical performance of the proposed antenna with respect to [22, 23] shows significance improvement in the gain, directivity and the radiation efficiency. This antenna also excludes from

the shorting post technique as reported in [23], which is the major fabrication challenge at the terahertz frequency. Future research will continue to push forward on all fronts, particularly in terahertz imaging system to increase the speed, bandwidth and resolution. With advances in coherent generation and application, it will be possible to develop arrays of the sources and detectors in imaging system to offer a new screening technology.

**Acknowledgements** Authors are sincerely thankful to the reviewers for critical comments and suggestions to improve the quality of the manuscript.

## References

1. Siegel, P.H.: THz instruments for space. *IEEE Trans. Antennas Propag.* **55**(11), 2957–2965 (2007)
2. Siegel, P.H.: THz technology in biology and medicine. *IEEE Trans. Microwave Theory Tech.* **52**(10), 2438–2448 (2004)
3. Pierewicz, R., Jacob, M., Koach, M., Schoebel, J., Kuner, T.: Performance analysis of future multigigabit wireless communication systems and THz frequency with highly directive antennas in indoor environments. *IEEE J. Sel. Top. Quantum Electron.* **14**(2), 421–430 (2008)
4. Galoda, S., Singh, G.: Fighting terrorism with terahertz. *IEEE Potentials Mag.* **26**(6), 24–29 (2007)
5. Gonzalo, R., Martinez, B.: The effect of dielectric permittivity on the properties of photonic band gap devices. *Microwave Opt. Tech. Lett.* **23**(2), 92–95 (1999)
6. Meade, R.D., Rappe, A.M., Brommer, K.D., Joannopoulos, J.D.: Nature of the photonic band gap devices. *J. Opt. Soc. Am. B* **10**, 328–332 (1993)
7. Gonzalo, R.: Enhanced patch-antenna performance by suppressing surface waves using photonic-band gap substrates. *IEEE Trans. Microwave Theory Tech.* **47**(11), 2131–2138 (1999)
8. Zhang, Z., Satpathy, S.: Electromagnetic wave propagation in periodic structures: Bloch wave solution of Maxwell equations. *Phys. Rev. Lett.* **65**(21), 2650–2653 (1990)
9. Ho, M.K., Chan, C.T., Soukoulis, C.M.: Existence of a photonic gap in periodic dielectric structures. *Phys. Rev. Lett.* **65**(25), 3152–3155 (1990)
10. Yang, H.Y.D., Alexopoulos, N.G., Yablonovitch, E.: Photonic band gap materials for high gain printed circuit antennas. *IEEE Trans. Antennas Propag.* **45**(1), 185–187 (1997)
11. Fernandes, H.C.C., da Rocha, A.R.B.: Analysis of antennas with PBG substrate. *Int. J. Infrared Millimeter Waves* **24**(7), 1171–1176 (2003)
12. Brown, E.R., Parker, C.D.: Radiation properties of a planar antenna on a photonic-crystal substrate. *J. Opt. Soc. Am. B* **10**(2), 404–407 (1993)
13. Dahele, J.S., Lee, K.F., Wong, D.P.: Dual-frequency stacked annular-ring microstrip antenna. *IEEE Trans. Antennas Propag.* **35**(11), 1281–1285 (1987)
14. Wang, J., Fralich, R., Wu, C., Litva, J.: Multifunctional aperture-coupled stacked antenna. *Electron. Lett.* **26**(25), 2067–2068 (1990)
15. Croq, F., Pozar, D.M.: Multi-frequency operation of microstrip antennas using aperture coupled parallel resonators. *IEEE Trans. Antennas Propag.* **40**(11), 1367–1374 (1992)
16. Richards, W.F., Davidson, S.E., Long, S.A.: Dual-band reactively loaded microstrip antenna. *IEEE Trans. Antennas Propag.* **33**(5), 556–560 (1985)
17. Davidson, S.E., Long, S.A., Richards, W.F.: Dual-band microstrip antenna with monolithic reactive loading. *Electron. Lett.* **21**(21), 936–937 (1985)
18. Croq, F., Pozar, D.M.: Millimeter-wave design of wide-band aperture-coupled stacked microstrip antennas. *IEEE Trans. Antennas Propag.* **39**(12), 1770–1776 (1991)
19. Lee, R.Q., Lee, K.F.: Gain enhancement of microstrip antennas with overlaying parasitic directors. *Electron. Lett.* **24**(11), 656–658 (1998)
20. Lee, R.Q., Lee, K.F.: Experimental study of two-layer electromagnetically coupled rectangular patch antenna. *IEEE Trans. Antennas Propag.* **38**(8), 1298–1302 (1990)
21. Sharma, A., Singh, G.: Design of single pin shorted three-dielectric-layered substrates rectangular patch microstrip antenna for communication systems. *Prog. Electromagn. Res. Lett.* **2**, 157–165 (2008)
22. Sharma, A., Dwivedi, V.K., Singh, G.: THz rectangular patch microstrip antenna design using photonic crystal as substrate. In: *Progress in Electromagnetic Research Symposium, Cambridge, USA, July 2–6, 2008*, pp. 161–165 (2008)
23. Sharma, A., Singh, G.: Rectangular microstrip patch antenna design at THz frequency for short distance wireless communication systems. *J. Infrared Millimeter Terahertz Waves* **30**, 1–7 (2009)
24. Kobayashi, M.: A Dispersive Formula Satisfying Recent Requirements in Microstrip CAD. *IEEE Trans. Microwave Theory Tech.* **36**(8), 1246–1250 (1988)
25. Poucel, R.A., Masse, D.J., Hartwig, C.P.: Correction to losses in microstrip. *IEEE Trans. Microwave Theory Tech.* **16**(12), 1064 (1968)
26. Wheeler, H.A.: Transmission-line properties of parallel strips separated by a dielectric sheet. *IEEE Trans. Microwave Theory Tech.* **6**(12), 1021–1027 (1968)